New Limit on the Low-Energy Antiproton/Proton Ratio in the Galactic Cosmic Radiation

S. P. Ahlen,[1] S. Barwick,[2] J. J. Beatty,[1] C. R. Bower,[3] G. Gerbier,[2] R. M. Heinz,[3] D. Lowder,[2] S. McKee,[4] S. Mufson,[5] J. A. Musser,[4] P. B. Price,[2] M. H. Salamon,[2],[a] G. Tarlé,[4] A. Tomasch,[1] and B. Zhou[1]

[1]*Physics Department, Boston University, Boston, Massachusetts 02215*
[2]*Physics Department, University of California, Berkeley, California 94720*
[3]*Physics Department, Indiana University, Bloomington, Indiana 47405*
[4]*Physics Department, University of Michigan, Ann Arbor, Michigan 48109*
[5]*Astronomy Department, Indiana University, Bloomington, Indiana 47405*
(Received 3 December 1987)

We describe the results of a balloon-borne apparatus searching for low-energy antiprotons in the Galactic cosmic rays. For energies less than 640 MeV at the top of the atmosphere, no cosmic-ray antiprotons were observed. This yields an upper limit to the $\bar{p}/p$ ratio of 4.6×10^{-5} at the 85% confidence level.

PACS numbers: 98.60.Ce, 14.80.Ly, 98.60.Ln

Conventional models of cosmic-ray propagation predict the production of secondary antiprotons ($\bar{p}$'s) through collisions of high-energy cosmic rays with the interstellar medium.[1] At several gigaelectronvolts the predicted $\bar{p}/p$ ratio is of the order 10^{-4} and is expected to decrease with increasing energy as $E^{-0.6}$. For energies less than 1 GeV, secondary production is suppressed and results in a $\bar{p}/p$ ratio less than 10^{-5}. Thus the report[2] in 1981 of a cosmic-ray $\bar{p}/p$ ratio of $(2.2\pm0.6)\times10^{-4}$ for the energy interval 130 to 320 MeV (corrected to the top of the atmosphere) appeared to demand either a novel mechanism for $\bar{p}$ production or a radical revision of our understanding of cosmic-ray propagation. Many models of both categories have since been offered.[3] Of particular interest is the suggestion that low-energy $\bar{p}$'s are to be expected as annihilation products of photinos,[4-6] or Higgsinos,[6,7] if these particles constitute the missing dynamical mass of the Galactic halo. Although the details of these models depend on unknown mass parameters, distinct $\bar{p}$ spectral features are predicted which, if observed, could be interpreted as support for the role of these annihilating particles as the dark matter in the Galaxy and the Universe. This Letter describes the results of a balloon experiment (PBAR) which we have recently performed to measure the low-energy $\bar{p}/p$ ratio.

A schematic of PBAR appears in Fig. 1. S1 and S2 are scintillators used to identify the charge and velocity of cosmic-ray particles. S1 consists of three segments (each having dimensions $100\times25\times2.54$ cm^3) of fast plastic scintillator (Bicron BC420); S2 consists of two such segments. Each end of each segment is viewed through a bent, twisted light pipe by a fast (Phillips Model XP2020) photomultiplier tube (PMT). A relativistic muon yields 50 photoelectrons per PMT. DT is a drift-tube hodoscope which is placed in the bore of a split-coil superconducting magnet having a central field of 9 kG and a field nonuniformity of $\simeq$20%. The magnet design permits particles to pass through DT without coming in contact with the Dewar flash. DT determines the sign of the charge and the rigidity of cosmic rays by measuring the particle trajectory in the magnetic field. In conjunction with measurements of charge and velocity this permits the complete identification of the particles passing through PBAR. DT consists of 323 drift tubes in sixteen planes having tubes parallel to the magnetic field and eight planes having tubes perpendicular to the field. Each tube is 1.27 cm in diameter with a 20-μm wire strung down the center. A 50-50 mixture of Ar-C_2H_6 flows serially through the 323 tubes at slightly higher than ambient pressure. The total wall thickness traversed by a particle passing through DT is 0.28 g/cm^2. CK, a 15-cm-thick water Cherenkov counter, was not used for the analysis of data presented here.

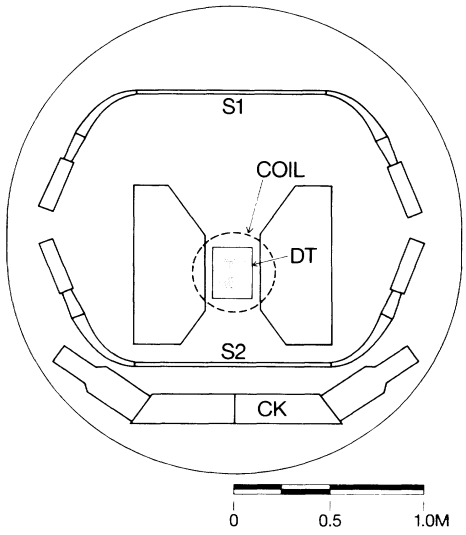

FIG. 1. Schematic of the PBAR instrument.

PBAR was flown in an aluminum shell by balloon from Prince Albert, Saskatchewan, on 13–14 August 1987. The environment during the flight was ideal, the temperature deviating from 20 °C by no more than a few degrees and the gondola pressure maintaining good stability near 1 atm. PBAR achieved an altitude of 36 km for a duration of 10 h 35 min. The latitude varied between 53° 18′ N and 54° 22′ N, and the longitude between 104° 55′ W and 108° 04′ W. Science and housekeeping data were telemetered to a ground station for recording and on-line display, and commands were sent to the instrument as necessary. Particle candidates were required to pass a two-level trigger. A fast trigger was generated by a coincidence between any S1 PMT and any S2 PMT, which gated the electronics. A subsequent slow trigger was required from DT (any tube in the top two planes and any tube in the bottom two planes) to complete digitization of the event, which was then telemetered to the ground. The efficiency of this trigger was determined to be nearly 100% in preflight tests with cosmic-ray muons. Magnetic tapes of data recorded during the flight were distributed to the four institutional groups, who performed independent analyses. The results described below correspond only to events with energy less than 620 MeV/amu in DT.

Figure 2 shows the S2-S1 time-of-flight (TOF) resolution and the DT spatial resolution as determined from the flight data. Event positions along the length of any scintillator can be determined by two independent methods. The most accurate method uses the DT vector formation to extrapolate an event position on the scintillator. A second method uses the time difference between the left and right PMT on each scintillator. The TOF standard deviation can be determined from the relation $\sigma_{\mathrm{TOF}} = (L/v)\sigma_{\Delta\tan\theta} = 160$ ps, where L is the separation of S1 and S2, $\Delta\tan\theta$ is the difference in track slopes as determined by DT vector information and PMT time differences in S1 and S2, and v is the effective propagation speed of light in the scintillators. Effective propagation speeds were determined from the measured slopes in plots of PMT time differences versus position extrapolated from DT. The width of the histogram in Fig. 2(a) was used to calculate that the PBAR timing resolution was 160 ps. Figure 2(b) shows the residuals of the drift tubes for fitted proton tracks in the magnetic field during the flight. The single-tube standard deviation is 109 μm averaged over all energies and angles.

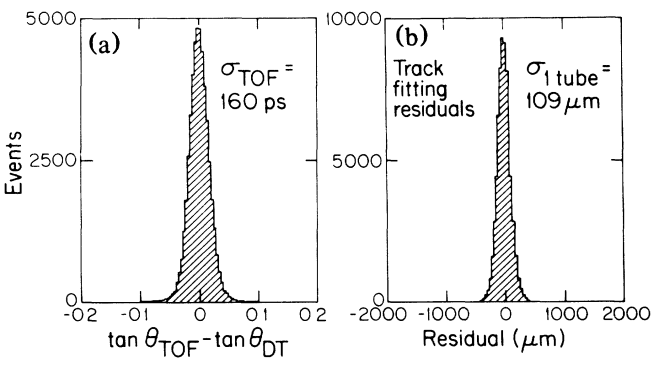

FIG. 2. (a) Histogram of track slope differences determined by drift tubes and scintillators. (b) Histogram of residuals of drift-tube position measurements.

In order to discriminate against particles with $|Z| > 1$, reduce backgrounds due to nuclear interactions and scattering, and maintain high efficiency for $\bar{p}$'s which annihilate in the detector, the following cuts were applied:

(1) Only one S1 segment has both PMT's triggered (eliminates showers).

(2) At least one S2 segment has two PMT's triggered (allows multiple hits due to annihilation pions produced in S2 and CK).

(3) The particle is downward moving (rejects albedo).

(4) At least one drift tube is hit in each of the top two and bottom two rows of DT, with at least six rows in both the top and bottom halves of DT parallel to **B** containing hits, and only one clean track is present in DT (clean trajectory data).

(5) The particle rigidity (from DT) is less than 1.5 GV and its speed is between $0.17c$ and $0.8c$ as determined by TOF (restricts energy range).

(6) The χ^2 for the fit of the track in the sixteen planes of tubes parallel to **B** is less than 41 (rejects scatters).

(7) The slopes of the track as measured by DT and the scintillators must be within 0.10 of each other (eliminates spurious TOF timing).

(8) The signals in the scintillator segments pointed to by the track in DT must exceed 100 photonelectrons (eliminates particles clipping scintillator corners), S1 $< 3\mathrm{S1}_{\mathrm{calc}}$ (eliminates $|Z| > 1$), and $\mathrm{S2} > \mathrm{S2}_{\mathrm{calc}}/6$ (eliminates corner clippers for large S2 pulse heights, but allows large signals for annihilation pions). The $\mathrm{S}_{\mathrm{calc}}$

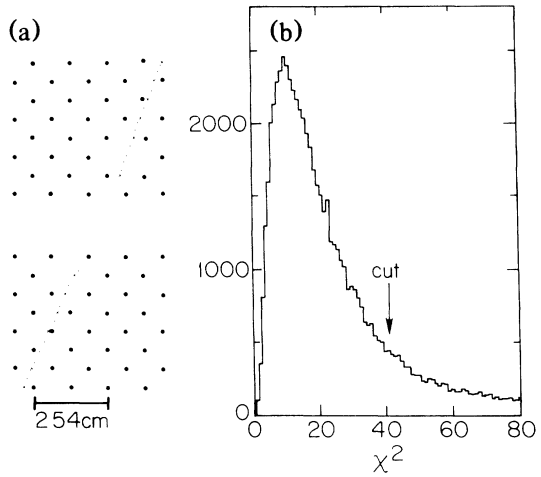

FIG. 3. (a) A track of a typical background event. (b) The χ^2 distribution for the fitted tracks.

values are those expected for a proton having the rigidity measured by DT.

An example of a hard-scatter background event is shown in Fig. 3(a). This is the track of a proton which scattered in the middle of DT, simulating the same sense of curvature as an antiproton. The χ^2 for this event is 76, and so it is rejected by our cut on goodness of fit at $\chi^2=41$, shown in Fig. 3(b).

For events which passed the above cuts, masses were calculated with the rigidity determined by DT and the velocity from TOF. Figure 4 shows the resulting mass histograms for positive and negative charge. Peaks for protons, positive and negative muons and/or pions, and possibly for negative and positive kaons are present. There are a total of 52000 protons in the mass range 600–1500 MeV/c^2. However, *there are no $\bar{p}$ candidates.* The mass spectrum for albedo (upward moving) protons is shown beneath the proton spectrum. Except for a slight shift in the mass peak, there is no evidence that these particles, which have the same sense of curvature as would $\bar{p}$'s, are treated any differently than downward moving protons. Furthermore, the ratio of negative to positive muons and/or pions is consistent with accelerator measurements.[8] Thus, it is apparent that there are no flaws in our track-fitting algorithms which would selectively remove $\bar{p}$'s from our data set. Nor can charge-sign asymmetry effects of detector response account for a bias against $\bar{p}$'s.[9]

In our calculating an upper limit to $\bar{p}/p$ from these data, the annihilation of $\bar{p}$'s in the atmosphere and instrument must be taken into account. A $\bar{p}$ which annihilates in the instrument (which would occur predominantly in CK) could be rejected in three ways: (i) multiple tracks in DT due to one or more secondary pions; (ii) multiple S1 slabs struck by one or more pions; and (iii) spurious S2 timing information for the S2 segment traversed by the $\bar{p}$, due to a pion's hitting the slab between its end and the $\bar{p}$ scintillation wave front. Mechanisms (i) and (ii) cause 6% of annihilations to be lost, while 5% are lost to (iii). Since 30% of $\bar{p}$'s annihilate in S2 or CK, the total correction to $\bar{p}/p$ is 1.03. A factor of 1.14 must be included to correct for $\bar{p}$'s which annihilate in the 8 g/cm^2 of material from the top of the atmosphere to the bottom of S1.[10] A factor of 1.13 must also be included to account for the enhancement of the proton flux due to secondary[11] and albedo protons at the top of the instrument, with an additional factor of 0.94 applied to account for protons absorbed in the atmosphere. The combined correction factor is 1.25, resulting in an 85%-confidence-level (C.L.) upper limit of $\bar{p}/p < 4.6 \times 10^{-5}$ at the top of the atmosphere in the energy range 205–640 MeV. The lower bound on the energy is due to the geomagnetic cutoff rigidity.

Solar-cycle modulation effects reduce the energy of cosmic rays entering the heliosphere[12,13] and are important at low energies.[14] The observed energy window for PBAR corresponds to 700–1135 MeV in interstellar

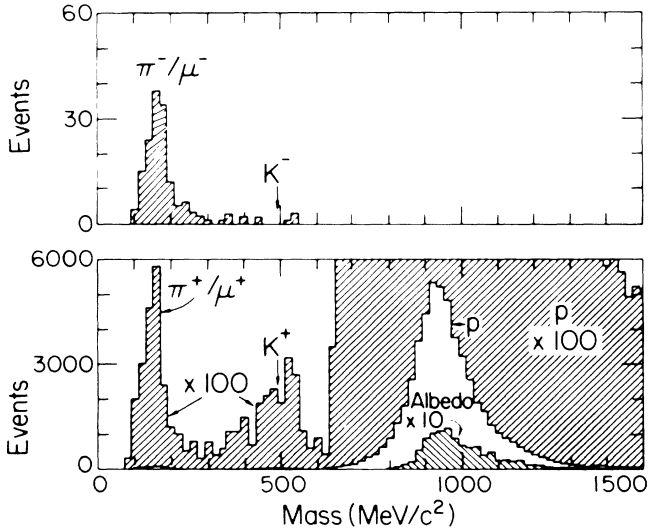

FIG. 4. Mass spectra for positive and negative singly charged particles. There are three histograms for the positive-curvature events. From top to bottom they are as follows: two for the downward-going particles at two different scales, and one for albedo particles at an expanded scale.

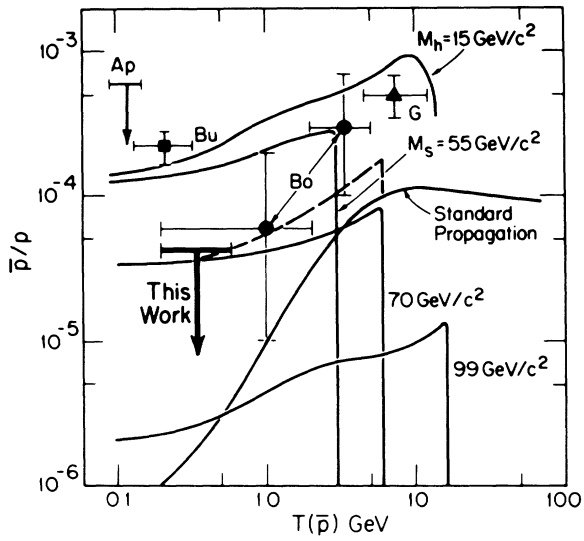

FIG. 5. Comparison of data with several models for the $\bar{p}/p$ ratio. The limits shown for this work are at the 85% confidence level so that they correspond to the upper limit of a 1σ error bar, Ap is from Ref. 17, Bo is from Ref. 19, Bu is from Ref. 2, and G is from Ref. 18. The standard propagation is a leaky-box calculation from Fig. 6 of Ref. 1b. Three curves for the photino model are shown, corresponding to photino masses of 3, 6, and 16 GeV/c^2, and scalar-fermion masses M_s of 55, 70, and 99 GeV/c^2, respectively. The Higgsino model (mass = 15 GeV/c^2) from Ref. 7 is also shown. These spectra have been modified to take solar modulation into account. The dashed line is the sum of the standard propagation and the 6-GeV photino curve.

space when estimated by the force-field approximation to solar modulation. For Ref. 2 the corresponding interval is 930–1120 MeV in interstellar space, allowing the two results to be directly compared. Satellite measurements from IMP-8 indicate no significant flux of solar protons above 100 MeV at the time of the PBAR flight.[15] Possible modulation effects which depend on charge sign,[16] although small, would tend to enhance the discrepancy between the present result and that of Ref. 2.

In Fig. 5 we compare data on $\bar{p}/p$ ratio with other data[2,17-19] and with several models. Each model has been corrected for the level of solar modulation present during our flight near solar minimum by integration of the spherically symmetric Fokker-Planck equations with a diffusion coefficient of the form given in Ref. 13 ($\phi = 500$ MV). We show Protheroe's standard cosmic-ray propagation model[1b] and several models involving the annihilation of exotic dark matter. The photino models require that photinos account for the missing mass of the Universe (with the assumption $\Omega = 1$), and for the dark matter in the galactic halo. The former constraint establishes a relation between the photino mass and the scalar fermion mass,[20] while the latter makes possible the calculation of $\bar{p}/p$ in the local interstellar medium.[5] This model cannot be correct unless the photino mass is greater than $\simeq 6$ GeV/c^2 and the scalar fermion mass is greater than $\simeq 70$ GeV/c^2. These values have not been excluded by accelerator searches[21] or by searches for high-energy neutrino emission from the Sun.[20]

Also shown in Fig. 5 is the ratio $\bar{p}/p$ for the Higgsino model proposed in Ref. 7, where Higgsinos of mass 15 GeV/c^2 account for the dark matter in the galactic halo. This model is inconsistent with our data, but would be consistent if the Higgsino mass were greater than 25 GeV, or if the mass density of the galactic halo were a factor of 2 smaller than that assumed in Ref. 7.

The results presented here represent the best limit to date on the ratio of antiprotons to protons in our galaxy. However, since the fraction of extragalactic cosmic rays in the neighborhood of the Earth at the energies considered here is likely to be no more than 2×10^{-5},[22] our results shed no light on the question of primary sources of antimatter outside of our galaxy.

This experiment was made possible by the efforts of personnel from the National Scientific Balloon Facility and by financial assistance from Boston University (B.U.), Indiana University (I.U.), and the University of Michigan (U.M.). We also acknowledge assistance from J. Bartlett, A. Buffington, R. Claxton, M. Gebhard, T. Karakashian, S. Lopez, H.-S. Park, J. Reynoldson, M. Solarz, and G. Turner. This work was supported by National Science Foundation Grants No. PHY-8519440 (B.U.), and No. PHY-8603225 and No. PHY-8702763 [University of California, Berkeley (U.C.B.)], U.S. Department of Energy Contract No. DE-AC02-76ER01112 (U.M.), NASA Contracts No. NGT-50014 (U.C.B.), No. NAS1-17820 (U.M.) and No. NAGW 1035 (I.U.), and Calspace Grants No. CS78-87 and No. CS08-86 (U.C.B.).

[a]Present address: Physics Department, University of Utah, Salt Lake City, UT 84112.

[1a]T. K. Gaisser and E. H. Levy, Phys. Rev. D **10**, 1731 (1974).

[1b]R. J. Protheroe, Astrophys. J. **251**, 387 (1981).

[2]A. Buffington, S. M. Schindler, and C. R. Pennypacker, Astrophys. J. **248**, 1179 (1981).

[3]S. A. Stephens and B. G. Mauger, Astrophys. Space Sci. **110**, 337 (1985); M. S. Turner, Nature (London) **297**, 379 (1982); F. W. Stecker, R. J. Protheroe, and D. Kazanas, Astrophys. Space Sci. **96**, 171 (1983); L. C. Tan and L. K. Ng, J. Phys. G **9**, 227 (1983); C. D. Dermer and R. Ramaty, Nature (London) **319**, 205 (1986).

[4]J. Silk and M. Srednicki, Phys. Rev. Lett. **53**, 624 (1984).

[5]F. W. Stecker, S. Rudaz, and T. F. Walsh, Phys. Rev. Lett. **55**, 2622 (1985).

[6]J. S. Hagelin and G. L. Kane, Nucl. Phys. B **B263**, 399 (1986).

[7]S. Rudaz and F. W. Stecker, University of Minnesota Report No. UMN-TH-606/87, 1987 (to be published).

[8]V. G. Grishin, Usp. Fiz. Nauk **127**, 51 (1979) [Sov. Phys. Usp. **22**, 1 (1979)].

[9]S. P. Ahlen, Rev. Mod. Phys. **52**, 121 (1980).

[10]T. Bowen and A. Moats, Phys. Rev. D **33**, 651 (1986).

[11]T. A. Tygg and J. A. Earl, J. Geophys. Res. **76**, 7445 (1971).

[12]L. J. Gleeson and W. I. Axford, Astrophys. J. **154**, 1011 (1968).

[13]M. Garcia-Munoz *et al.*, in *Proceedings of the Nineteenth International Cosmic Ray Conference, La Jolla, California, 1985,* edited by F. C. Jones, J. Adams, and G. Mason, NASA Conference Publication No. 2376 (U.S. GPO, Washington, D.C., 1985), Vol. 4, p. 409.

[14]J. S. Perko, Astron. Astrophys. **184**, 119 (1987).

[15]K. R. Pyle, private communication.

[16]P. Evenson, M. Garcia-Munoz, P. Meyer, K. R. Pyle, J. A. Simpson, Astrophys. J. **275**, L15 (1983).

[17]M. V. K. Apparao, Can. J. Phys. **46**, S654 (1968).

[18]R. L. Golden *et al.*, Phys. Rev. Lett. **43**, 1196 (1979).

[19]E. A. Bogomolov *et al.*, in *Proceedings of the Sixteenth International Cosmic Ray Conference, Kyoto, Japan, 1979,* edited by S. Miyake (Univ. of Tokyo Press, Tokyo, 1979), Vol. 1, p. 330; E. A. Bogomolov *et al.*, in *Proceedings of the Twentieth International Cosmic Ray Conference, Moscow, U.S.S.R., 1987,* edited by V. A. Kozyarivsky *et al.* (Nauka, Moscow, 1987).

[20]T. K. Gaisser, G. Steigman, and S. Tilav, Phys. Rev. D **34**, 2206 (1986).

[21]R. M. Barnett, H. F. Haber, and G. L. Kane, Nucl. Phys. **B267**, 625 (1986).

[22]S. P. Ahlen, P. B. Price, M. H. Salamon, and G. Tarlé, Astrophys. J. **260**, 20 (1982).

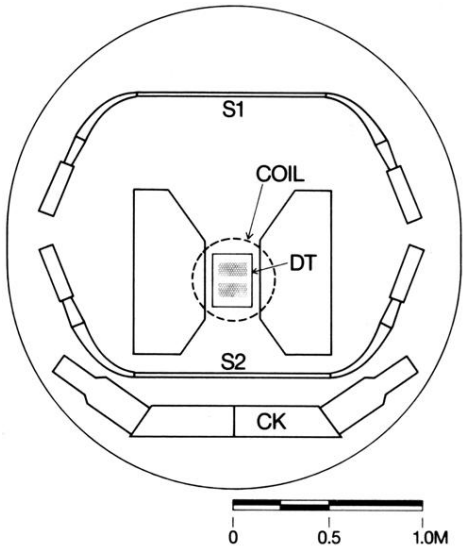

FIG. 1. Schematic of the PBAR instrument.